

Enhancement of the Rate Capability of Graphite via the Introduction of Boron–oxygen Functional Groups

Jae-Seong Yeo¹, Tae-Hwan Park¹, Min-Hyun Seo², Jin Miyawaki², Isao Mochida³, Seong-Ho Yoon^{1,2,*}

¹ Interdisciplinary Graduate School of Engineering Sciences, Kyushu University, Kasuga, Fukuoka 816-8580, Japan

² Institute for Materials Chemistry and Engineering, Kyushu University, Kasuga, Fukuoka 816-8580, Japan

³ Research and Education Centers of Carbon Resources, Kyushu University, Kasuga, Fukuoka 816-8580, Japan

*E-mail: yoons@cm.kyushu-u.ac.jp

Received: 27 September 2012 / Accepted: 29 November 2012 / Published: 1 January 2013

The rate capability of graphite was enormously enhanced by introducing (meta)boric acid containing boron–oxygen groups onto its surface. Sample that had been heat-treated at 1000°C exhibited two times larger capacity at even 5C discharge rate than those of the as-received sample. The presence of (meta)boric acid on the surface of graphite reduced the resistance and capacitance of surface films related to lithium ion migration and charge transfer resistance. However, the samples heat-treated at temperatures above 1500°C showed no improvements in rate capability due to the disappearance of boron–oxygen groups from the graphite surface.

Keywords: Graphite, (Meta)boric acid, Rate capability, Lithium-ion battery

1. INTRODUCTION

Recently, research into large-scale Li-ion batteries has been ramped up for applications in electric vehicles and as large-scale backup power supplies. Such applications require carbonaceous anode materials with high rate capabilities and long lifetimes. Graphite is still considered an important anodic material in Li-ion batteries due to its high reversible capacity, flat voltage profile, good cyclability, and low cost. However, the rate capability of graphite is not sufficient for high-power density batteries. Rate capability can be increased by reducing the solid-state diffusion path of Li ions by using, for example, nano-structured materials such as carbon nanofibers [1], and by increasing the ion diffusivity and electronic conductivity through the deposition of metals such as Sn, Al, and Ni [2–

4] or by coating with conductive polymers such as polypyrrole [5]. Kottegoda et al. reported that zirconia-treated graphite exhibits a stable capacity at relatively high charge-discharge rates. This effect is related to the enhancement of the passivating properties of in situ surface films by the porous zirconia crystalline film, resulting in the suppression of anode degradation upon cycling [6].

Boron doping is usually used to enhance the degree of graphitization in non-graphitic carbonaceous materials such as pitch and pitch-based carbon fibers. In these cases, boron is substitutionally incorporated between graphene layers and in defects [1,7]. As a result, charge capacity is enhanced by allowing more Li-ion intercalation. Kurita suggested that boron-substituted, disordered carbon atoms could more easily accept electrons from absorbed Li atoms due to the creation of a lower electron-acceptor level caused by boron substitution [8]. Thus, the adsorption energy of a Li atom would be largely enhanced by the substitution of carbon atoms by boron atoms [8]. However, to date, boron-related research has focused only on increasing the degree of graphitization in disordered carbon systems and their lithium intercalation capacity.

This study investigated the effects of boron–oxygen groups on the rate capability of graphite. Heat treatment temperature was adjusted to investigate structural and compositional changes in boron compounds and to determine the optimum conditions for creating the highest possible rate capability in graphite.

2. EXPERIMENTAL

2.1. Introduction of boron-oxygen groups onto the surface of graphite

Graphite (Hitachi Chemical) was used as received. Boric acid was introduced onto the surface of graphite by ball-milling graphite with H_3BO_3 (99.99% trace metals basis; Sigma-Aldrich), a precursor of boric acid, with subsequent heat treatment. The amount of added boron was 5 wt%. Graphite, boric acid, and zirconia balls (10 mm in diameter) were placed in a bottle with a ball-to-weight ratio of 22.5. Ball-milling was performed on a V-IML planetary mill at a rotation speed of 120 rpm for 24 h. The boric acid-mixed graphite was then heat-treated at different temperatures from 1000°C to 2400°C for 10 min.

2.2. Characterization

The carbon, hydrogen, and nitrogen contents of the samples were measured by elemental analysis. Crystallographic parameters were measured by X-ray diffraction (XRD, Ultima-III, Cu $\text{K}\alpha$; Rigaku). Structural changes associated with boric acid were investigated by Fourier transform infrared spectroscopy (FTIR, MB-series; Bomen) from 4000 to 400 cm^{-1} at a resolution of 4 cm^{-1} .

Electrochemical properties, including charge/discharge measurements, were performed using CR2032 two-electrode coin cells. Li metal foils were used as the counter and reference electrodes. The working electrode was prepared by mixing 90 wt% active material, 5 wt% styrene butadiene rubber (SBR), and 5 wt% carboxymethyl cellulose (CMC) in distilled water. The mixed slurry was coated

onto a copper foil and then dried in a vacuum oven at 100°C for 12 h. The electrolyte solution was 1 M LiPF₆ dissolved in ethylene carbonate (EC)/diethyl carbonate (DEC) (1:1 vol%; Kishida Chemical). The assembled coin cells were charged at a 0.1C rate and discharged at different rates from 0.1C to 5.0C between 0.003 and 1.5 V versus Li/Li⁺ (Toscat-3100; Toyo System) to determine rate capability (assuming 1.0C = 372 mA g⁻¹) at room temperature. Electrochemical impedance spectroscopic (EIS) studies were performed by applying a small perturbation voltage of 5 mV in the frequency range of 100 kHz to 100 mHz at 0.9 V.

3. RESULTS AND DISCUSSION

3.1. Physical properties of boron-oxygen groups introduced graphite

Fig. 1 shows the elemental composition of as-received, as-mixed, and heat-treated graphite samples. The carbon content of as-received graphite was 99.96%. The as-mixed graphite and the sample that had been heat-treated at 1000°C had carbon contents of 74.00% and 74.72%, respectively. Carbon content increased after heat treatments above 1500°C. The hydrogen content of the as-received graphite was 0.06%, which increased up to 1.23% and 0.90% in the as-mixed graphite and the sample that had been heated to 1000°C, respectively. Hydrogen content decreased after heat treatments above 1500°C. Boric acid remained in the as-mixed and 1000°C heat-treated graphites.

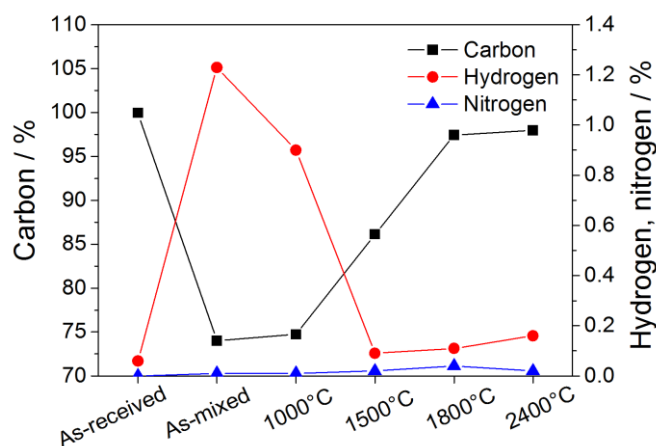


Figure 1. Carbon, hydrogen, and nitrogen contents of as-received, as-mixed, and heat-treated graphites.

Fig. 2 shows XRD profiles of the as-received, ball-milled, as-mixed, and heat-treated graphites. All samples exhibited sharp diffraction peaks near 26.6°, corresponding to the (002) crystallographic plane. This is consistent with the high degree of graphitization in graphite. For as-mixed graphite, a peak corresponding to the mixed boric acid was observed at 27.9° as indicated in Fig. 2(a). This peak disappeared following heat treatments above 1000°C. The boric acid present on the 1000°C and 1200°C heat-treated graphites may have been converted to another type of metaboric acid. Diffraction

peaks originating from boron carbide, which does not contribute to the electrochemical reaction [1], were observed at 35.0° and 37.8° for graphites that had been heat-treated at temperatures above 1500°C .

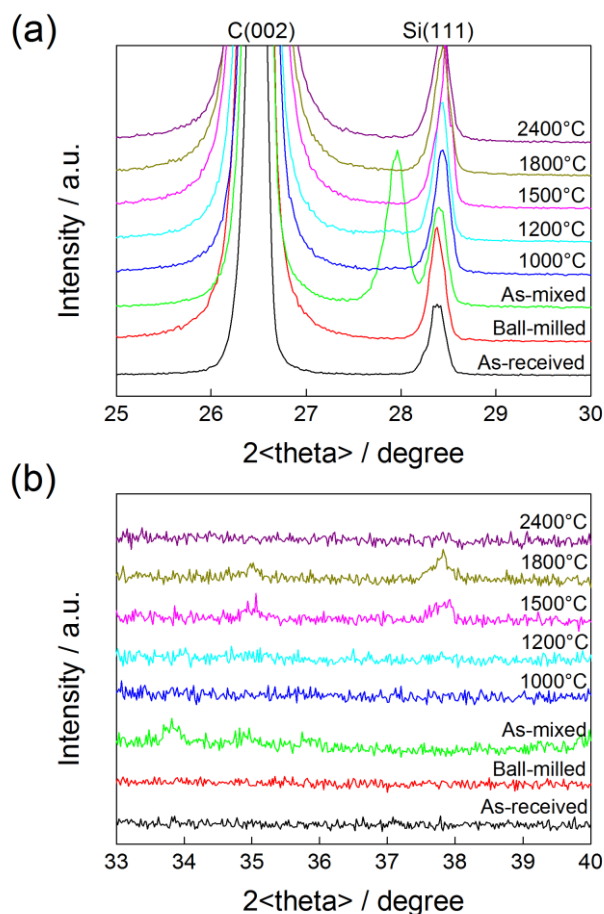


Figure 2. XRD profiles of (a) as-received, ball-milled, as-mixed, and heat-treated graphites. An enlarged view between 33° and 40° is shown in (b).

FTIR absorption spectroscopy was used to investigate structural changes associated with boric acid on the surface of graphite as a function of heat treatment temperature. FTIR spectra of ball-milled, as-mixed, and heat-treated graphites are shown in Fig. 3. Peaks were observed at 3200 cm^{-1} , $1396\text{--}1476\text{ cm}^{-1}$, 1195 cm^{-1} , and 780 cm^{-1} , corresponding to the O–H stretching band, asymmetric B–O stretching band, in-plane B–OH bending, and out-of-plane B–OH bending, respectively of boric acid [9]. All of these characteristic peaks were present in the spectra of the as-mixed and 1000°C and 1200°C heat-treated graphites but were absent from the spectra of graphites that had been heated above 1500°C . This provides further evidence that boric acid was removed from the surface at temperatures greater than 1500°C . As boric acid is heated, it converts to metaboric acid, then tetraboric acid, and finally to boron trioxide. The melting and boiling points of boron trioxide are 450°C and 1860°C , respectively, and the compound sublimates at 1500°C . Evaporated boron atoms can substitutionally incorporate between with carbon atoms or in defect sites within the graphitic planes of graphite. Fig.

3(b) shows the molecular structural changes in boric acid as a function of heat treatment temperature. The added boron likely exists as boric acid in the as-mixed graphite and as metaboric acid following heat treatment at 1000°C and 1200°C. Absorption peaks at 1579 cm⁻¹ and 2920 cm⁻¹, corresponding to an aromatic C=C stretching band and a C–H asymmetric stretch band [10,11], respectively, appear in the FTIR spectra of graphites that had been heat-treated above 1500°C. The as-received graphite was coated with pitch that was most likely graphitized above 1500°C, giving rise to the aromatic C=C stretching band. The peak at 1265 cm⁻¹, which corresponds to boron carbide, also appeared in samples that had been heated above 1500°C [12]. The existence of (meta)boric acid was confirmed by elemental analysis, and was observed in the FTIR spectra of the as-mixed graphite and in the spectra of samples that had been heat-treated at 1000°C and 1200°C.

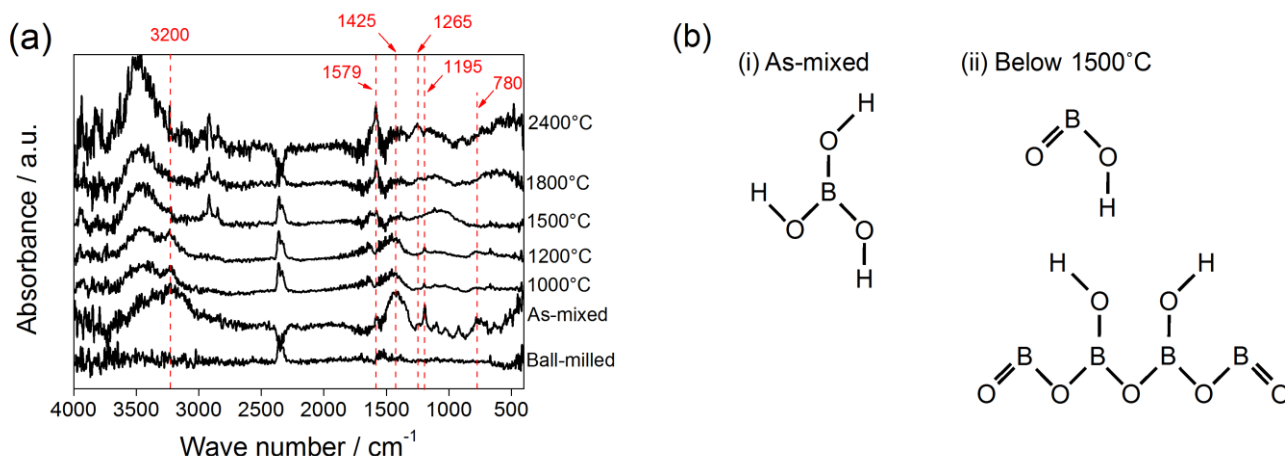


Figure 3. (a) FTIR spectra of ball-milled, as-mixed, and heat-treated graphites. (b) Molecular structural changes of boric acid adsorbed on graphite are shown as a function of heat treatment temperature.

3.2. Electrochemical properties of boron-oxygen groups introduced graphite

Fig. 4(a) and (b) shows the charge/discharge profiles of as-received, ball-milled, as-mixed, and heat-treated graphites at the third cycle, which consisted of a charge/discharge at 0.1C between 0.003 V and 1.5 V versus Li/Li⁺. The as-mixed and 1000°C and 1200°C heat-treated graphites exhibited more definite plateaus than the as-received, ball-milled, and heat-treated graphites above 1500°C, with voltages of 200, 114, and 76 mV for charge and 109, 145, and 226 mV for discharge, respectively [13,14]. Note that Li-ion de-intercalation occurred at lower potentials in the as-mixed and 1000°C and 1200°C heat-treated graphites than in the as-received, ball-milled, and graphites that had been heat treated above 1500°C. This suggests that (meta)boric acid, which provides boron–oxygen groups on the surface of the graphite anode, may act as a port for lithium ion migration and an intermediate reservoir of lithium ions when they intercalate or de-intercalate the graphite anode. Fig. 4(c) shows the rate capability of the as-received, ball-milled, as-mixed, and heat-treated graphites at different discharge rates from 0.1C to 5.0C. The as-mixed and 1000°C and 1200°C heat-treated graphites

exhibited a higher rate performance than the as-received and graphites that had been heat-treated above 1500°C.

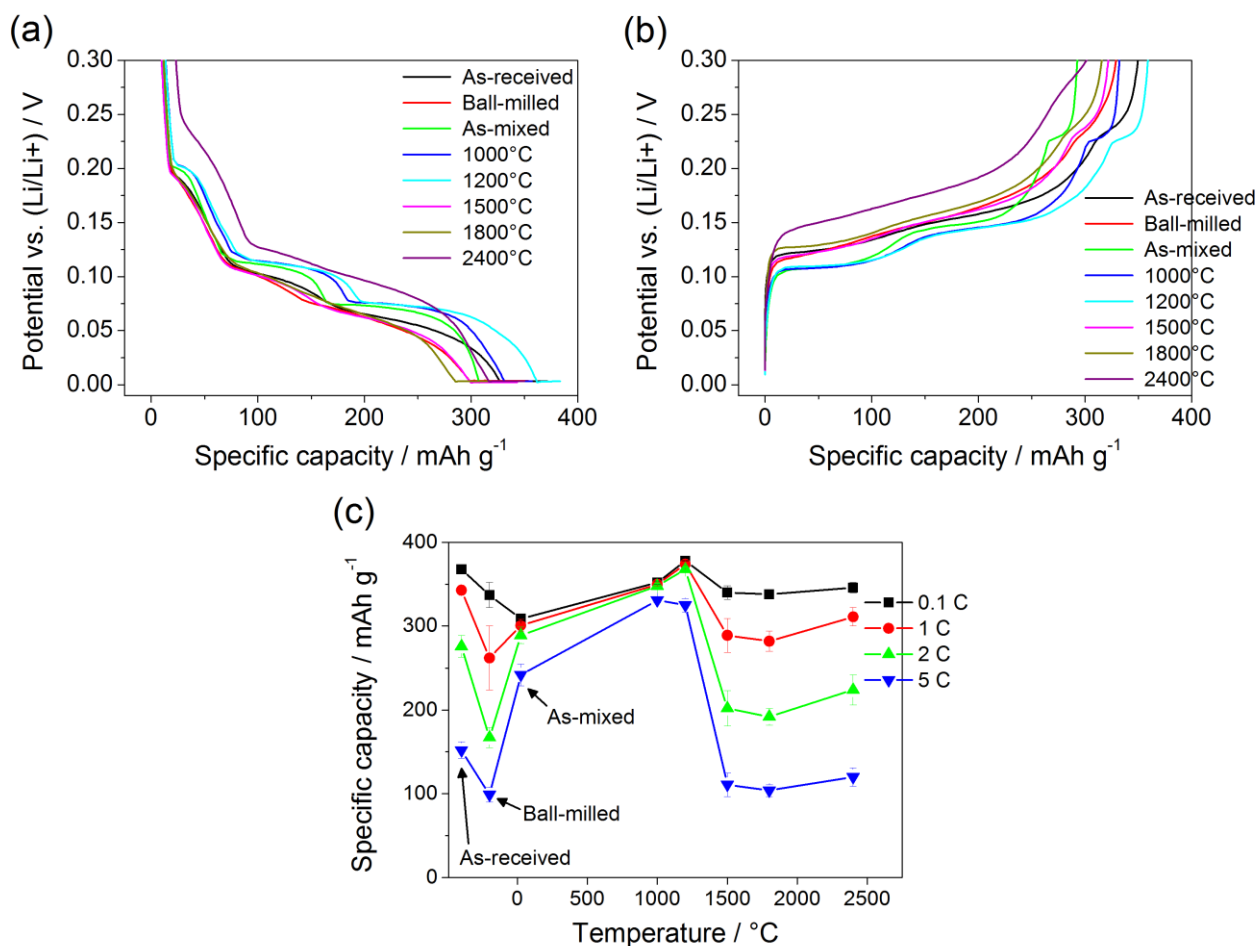


Figure 4. (a), (b) Charge/discharge profiles (third cycle), and (c) rate capabilities of as-received, ball-milled, as-mixed, and heat-treated graphites.

Fig. 5(a) and (b) show typical Nyquist plots of the as-received, ball-milled, as-mixed, and heat-treated graphites discharged to 0.9 V. The measured impedance data over the entire frequency range can be analyzed using the equivalent circuit shown in Fig. 5(b) [15]. Fig. 5(c) and (d) shows typical parameters for the high- and medium-frequency range determined from the best-fit curve. For the as-mixed and 1000°C and 1200°C heat-treated graphites, the resistance values calculated over the high-frequency range, which primarily characterize the migration of lithium ions through the multilayered surface films, decreased as shown in Fig. 5(c). This means that lithium ions could move relatively easily in and out of the surface films. As discussed above, (meta)boric acid on the surface of the graphite anode may act as a port for lithium ion migration. Can et al. [16] reported that the ionic conductivity of lithium metaborate (LiBO₂) is as high as 10^{-7.1} S cm⁻¹ and can increase by one order of magnitude with the addition of lithium fluoride. Fig. 5(d) shows the change in charge transfer resistance between the surface films and the graphite anode as a function of heat treatment temperature.

The as-mixed and 1000°C and 1200°C heat-treated graphites exhibited a lower charge transfer resistance than the as-received, ball-milled, and other graphites heat-treated above 1500°C. The excellent performance observed at various discharge rates may be attributable to the (meta)boric acid on the surface of the graphite anode.

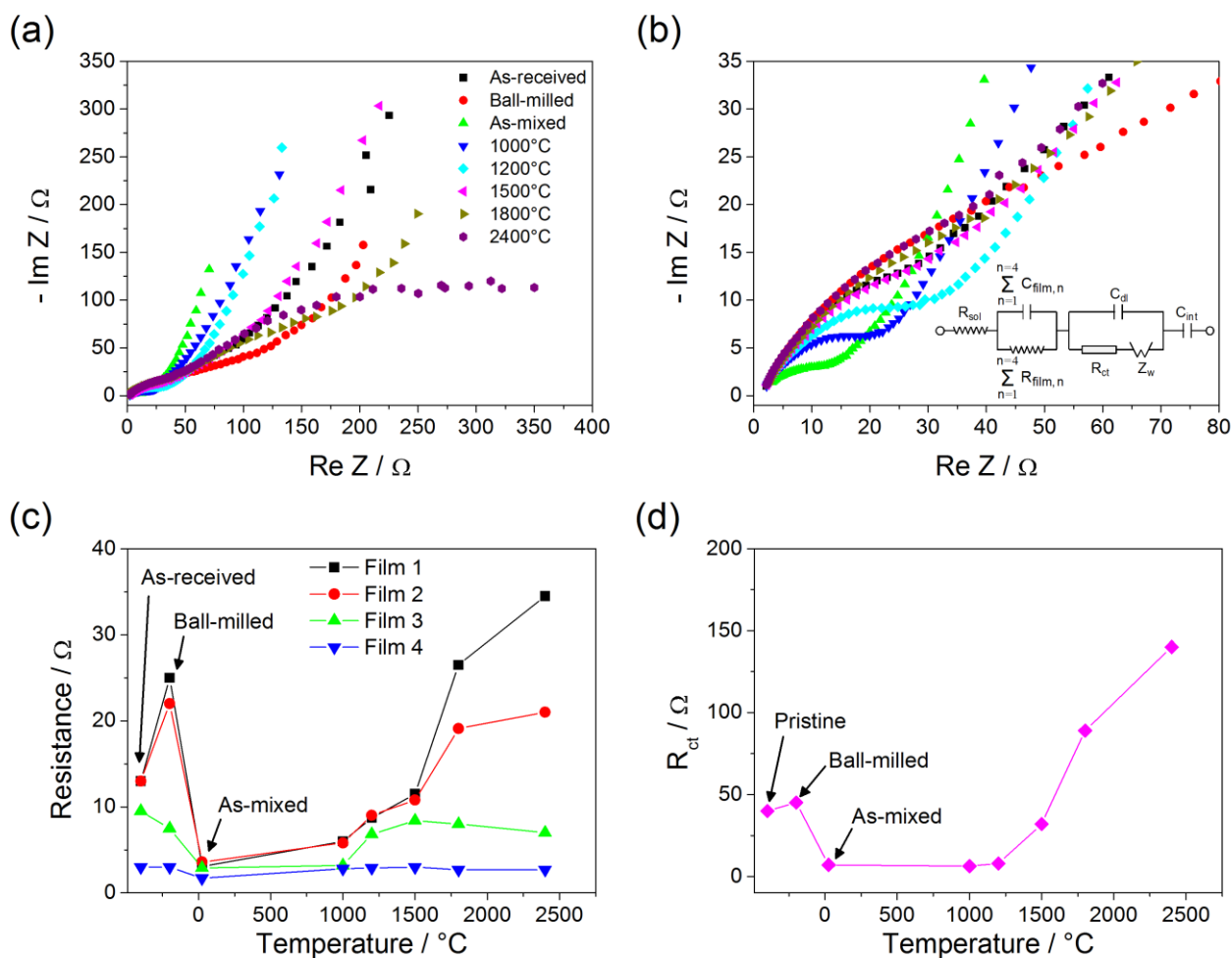


Figure 5. Typical Nyquist plots of the (a) as-received, ball-milled, as-mixed, and heat-treated graphites discharged to 0.9 V are shown with (b) an enlarged view of the high-frequency region and the equivalent circuit analog and typical parameters obtained by fitting the equivalent circuit to the experimental data: (c) resistance of the surface films and (d) the charge transfer resistance between the surface film and the graphite anode.

4. CONCLUSIONS

The rate capability of graphite was enhanced by introducing (meta)boric acid, which contains boron–oxygen groups, onto the surface of graphite. The introduction was made by ball-milling and subsequent heat treatment at temperatures below 1500°C. Samples that had been heat-treated at 1000°C exhibited two times higher rate performance than the as-received and graphites that had been heat-treated above 1500°C. AC impedance measurements showed that this enhancement may have

resulted from the reduction in surface film resistance and charge transfer resistance facilitated by the introduction of (meta)boric acid onto the surface of the graphite sample. Investigations are currently under way to elucidate the mechanism by which (meta)boric acid improves the rate capability of graphite.

ACKNOWLEDGMENTS

The authors would like to thank Mitsubishi Corporation for financial support and Prof. Jyongsik Jang and Mr. Sphoon Min of Seoul National University for their help with FTIR measurements. The authors are also very appreciative to Hitachi Chemical Co., Ltd. for supplying the graphite samples.

References

1. H. Fujimoto, A. Mabuchi, C. Natarajan and T. Kasuh, *Carbon*, 40 (2002) 567.
2. B. Veeraraghavan, A. Durairajan, B. Haran, B. Popov and R. Guidotti, *J. Electrochem. Soc.*, 149 (2002) A675.
3. S. Kim, Y. Kodoma, H. Ikuta, Y. Uchimoto and M. Wakihara, *Electrochem. Solid-State Lett.*, 4 (2001) A109.
4. L. Shi, Q. Wang, H. Li, Z. Wang, X. Huang and L. Chen, *J. Power Sources*, 102 (2001) 60.
5. B. Veeraraghavan, J. Paul, B. Haran and B. Popov, *J. Power Sources*, 109 (2002) 377.
6. I.R.M. Kottegoda, Y. Kadoma, H. Ikuta, Y. Uchimoto and M. Wakihara, *Electrochem. Solid-State Lett.*, 5 (2002) A275.
7. M. Endo, C. Kim, T. Karaki, Y. Nishimura, M.J. Matthews, S.D.M. Brown and M.S. Dresselhaus, *Carbon*, 37 (1999) 561.
8. N. Kurita, *Carbon*, 38 (2000) 65.
9. Y. Mulazim, C. Kizilkaya and M.V. Kahraman, *Polym. Bull.*, 67 (2011) 1741.
10. I.Y. Jeon, E.K. Choi, S.Y. Bae and J.B. Baek, *Nanoscale Res. Lett.*, 5 (2010) 1686.
11. A.M. Puziy, O.I. Poddubnaya, A. Martinez-Alonso, F. Suarez-Garcia and J.M.D. Tascon, *Carbon*, 43 (2005) 2857.
12. Z. Han, G. Li, J. Tian and M. Gu, *Mater. Lett.*, 57 (2002) 899.
13. J.R. Dahn, *Phys. Rev. B*, 44 (1991) 9170.
14. T. Ohzuku, Y. Iwakoshi and K. Sawai, *J. Electrochem. Soc.*, 140 (1993) 2490.
15. M.D. Levi and D. Aurbach, *J. Phys. Chem. B*, 101 (1997) 4630.
16. N. Can, S. Badilescu, F.E. Girouard and V. Truong, *Solid State Ionics*, 78 (1995) 231.